ANNALES
DE LA FACULTÉ
DES SCIENCES
DE
TOULOUSE
Mathématiques

SEBASTIAN BAADER, MASAHARU ISHIKAWA

Legendrian graphs and quasipositive diagrams

Tome XVIII, n° 2 (2009), p. 285-305.

<http://afst.cedram.org/item?id=AFST_2009_6_18_2_285_0>

Annales de la Faculté des Sciences de Toulouse Vol. XVIII, n° 2, 2009
pp. 285–305

Legendrian graphs and quasipositive diagrams

Sebastian Baader[1] and Masaharu Ishikawa[2]

Dedicated to Professor Norbert A'Campo
on the occasion of his 65th birthday

Abstract. — In this paper we clarify the relationship between ribbon surfaces of Legendrian graphs and quasipositive diagrams by using certain fence diagrams. As an application, we give an alternative proof of a theorem concerning a relationship between quasipositive fiber surfaces and contact structures on S^3. We also answer a question of L. Rudolph concerning moves of quasipositive diagrams.

Résumé. — Nous étudions ici la relation entre les surfaces de ruban associées aux graphs legendriens et les diagrammes quasi-positifs. Comme application, nous donnons une preuve élémentaire qu'une surface fibrée est quasi-positive, si et seulement si elle porte la structure de contact standard dans S^3. Nous répondons aussi à une question de L. Rudolph concernant les mouvements des surfaces quasi-positives.

1. Introduction

A link is called *quasipositive* if it has a diagram which is the closure of a product of conjugates of the positive generators of the braid group. If the product consists only of words of the form

$$\sigma_{i,j} = (\sigma_i \cdots \sigma_{j-2})\sigma_{j-1}(\sigma_i \cdots \sigma_{j-2})^{-1}$$

(*) Reçu le 23/08/06, accepté le 23/01/08
(1) Department of Mathematics, ETH Zürich, Switzerland
sebastian.baader@math.ethz.ch
(2) Mathematical Institute, Tohoku University, Sendai, 980-8578, Japan
ishikawa@math.tohoku.ac.jp

then the link obtained as its closure is called *strongly quasipositive.* Let b be the braid index of a braid diagram of a strongly quasipositive link. The link spans a canonical Seifert surface consisting of b copies of disjoint parallel disks with a band for each $\sigma_{i,j}$, for example see the diagram on the left in Figure 1. We call such a diagram of a Seifert surface a *quasipositive diagram* and each band a *positive band.* We say a Seifert surface is *quasipositive* if it has a quasipositive diagram. On the right in Figure 1, the quasipositive diagram is represented by using a graph, which is called a *fence diagram.*

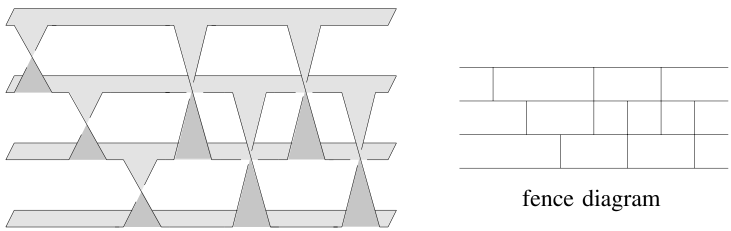

Figure 1. — An example of quasipositive surface.
The boundary is the knot 10_{145} in Rolfsen's notation [?].

To relate fence diagrams to contact topology, we replace each endpoint of vertical lines as shown in Figure 2 and call the obtained diagram its *cusped fence diagram.* A cusped fence diagram is regarded as a front projection of a Legendrian graph. We will see that the Legendrian ribbon of this Legendrian graph is the quasipositive surface of the fence diagram (Lemma 2.1). Conversely, when a front projection of a Legendrian graph is given, we can make a fence diagram whose quasipositive surface is a Legendrian ribbon of the given Legendrian graph. In particular, the Legendrian ribbon of a Legendrian graph in $\mathbb{R}^3$ with the standard contact structure is a quasipositive surface (Theorem 2.2).

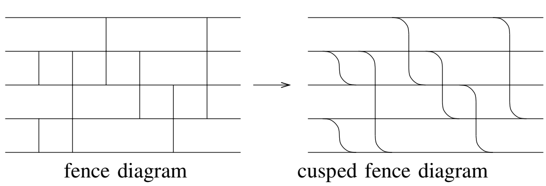

Figure 2. — From a fence diagram to a cusped fence diagram,
which is a front projection of a Legendrian graph.

As an application, we give an alternative proof of [?, Proposition 2.1 (1)⇔(2)] which states that a fiber surface is quasipositive if and only if it supports the standard contact structure on S^3 (Theorem **??**). The proof in [?] is based on the work of E. Giroux [?] and L. Rudolph [?], and uses plumbings. Hence it requires the affirmative answer to J. Harer's conjecture [?] due to Giroux and N. Goodman [?, ?]. In our proof, one direction follows from the fence diagram argument and the other one is done according to an argument in [?]. In particular, both directions do not need plumbings.

Next we study Legendrian isotopy moves of Legendrian graphs using moves of quasipositive surfaces. In [?], Rudolph introduced moves of quasipositive diagrams named *inflations, deflations, slips, slides, twirls and turns.* These moves are summarized in Figure 3. The same figures can be found in his paper [?] with more precise definitions. In his notation, we only consider the case where the signs ε assigned to bands are positive. There is a remark about these definitions, see Remark ?? below. We will prove that all Legendrian isotopy moves of Legendrian graphs are expressed by inflations, deflations, slips and slides of fence diagrams (Theorem ??).

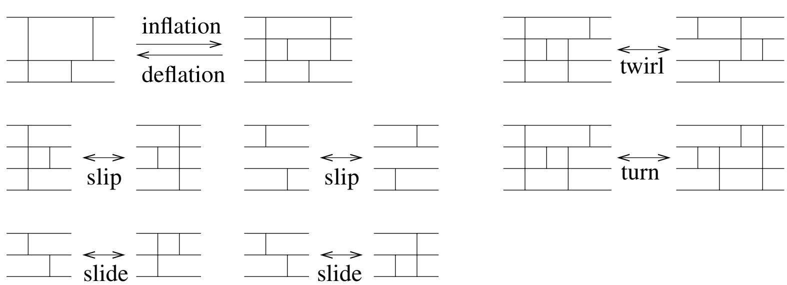

Figure 3. — Rudolph's moves of quasipositive diagrams.
Each positive band may pass over several horizontal lines.

In the last two sections we study quasipositive annuli. We first prove that the moves of fence diagrams of quasipositive annuli correspond to Legendrian isotopy moves (Theorem ??). It is important to remark that the same assertion is not true for quasipositive surfaces. Secondly, we study the Thurston-Bennequin invariant and the rotation number of fence diagrams of quasipositive annuli, which are defined by those of cusped fence diagrams. We prove that the Thurston-Bennequin invariant and the rotation number of a fence diagram of a quasipositive annulus are invariant under inflations, deflations, slips, slides, twirls and turns (Theorem ??). As a corollary, we conclude that there exists a quasipositive surface with two different quasipositive diagrams which are not related by inflations, deflations, slips, slides, twirls and turns. This answers a question of Rudolph in [?, Remark on p.263].

From the results in this paper, we conclude that there exist surjective, non-injective maps

$$\begin{aligned}\{\text{trivalent Legendrian ribbons}\}_{/\sim} &\to \{\text{quasipositive diagrams}\}_{/\sim}\\ &\to \{\text{quasipositive surfaces}\}_{/\sim},\end{aligned}$$

where $\{\text{trivalent Legendrian ribbons}\}_{/\sim}$ is the class of trivalent Legendrian graphs up to Legendrian isotopy, $\{\text{quasipositive diagrams}\}_{/\sim}$ is the class of quasipositive diagrams up to inflations, deflations, slips, slides, twirls and turns, and $\{\text{quasipositive surfaces}\}_{/\sim}$ is the class of quasipositive surfaces up to ambient isotopy.

This paper is organized as follows. In Section 2, we introduce the notion of front projections in backslash position and prove that a Legendrian ribbon is a quasipositive surface. In Section 3, we give an alternative proof of Hedden's proposition. Section 4 is devoted to Theorem **??** and Section 5 is devoted to Theorem **??**. In Section 6, we introduce the Thurston-Bennequin invariant and the rotation number of a fence diagram of a quasipositive annulus and prove their invariance under the moves of fence diagrams.

2. Legendrian graphs and quasipositive diagrams

The standard contact structure ξ_{st} on $\mathbb{R}^3$ is the kernel of the 1-form $dz + xdy$. A *Legendrian graph* is a finite graph consisting of edges and vertices such that each edge is Legendrian, i.e., tangent to the 2-plane field ξ_{st} everywhere. The graph may have a simple closed curve component, which we also call an edge for convenience. The image of the projection of a Legendrian graph Γ onto the yz-plane is called a *front projection* of Γ. This image is an immersed graph with cusps and without vertical tangencies. We call the image of each vertex also a vertex. If Γ is in general position, its front projection has only node and cusp singularities, and the edges adjacent to each vertex have the same tangency. We call such a Γ a *generic front projection*. For each node, we regard the arc with smaller slope as the strand passing over the other arc. Then the figure obtained becomes a graph diagram of Γ.

A *Legendrian ribbon* R of a Legendrian graph Γ in $(\mathbb{R}^3, \xi_{st})$ is a smoothly embedded surface in S^3 such that

(1) Γ is in the interior of R and R retracts onto Γ,

(2) for each $x \in \Gamma$, the 2-plane of ξ_{st} at x is tangent to R, and

(3) for each $x \notin \Gamma$, the 2-plane of ξ_{st} at x is transverse to R.

The notion of a ribbon of a Legendrian graph appears in [**?**] to prove the existence of an open book decomposition compatible with a given contact structure on a 3-manifold, see [**?**, **?**].

Regard a cusped fence diagram as a front projection, then the corresponding quasipositive diagram retracts onto the preimage of the cusped fence diagram. We call this preimage the *Legendrian core graph* of the quasipositive diagram.

LEMMA 2.1. — *A quasipositive diagram can be regarded as a Legendrian ribbon of its Legendrian core graph.*

Proof Set the b copies of disjoint parallel disks in $\mathbb{R}^3$ parallel to the xy-plane and attach the positive bands in the region $x > 0$ as shown in Figure 4. This figure shows that this surface is a Legendrian ribbon of the Legendrian core graph. $\square$

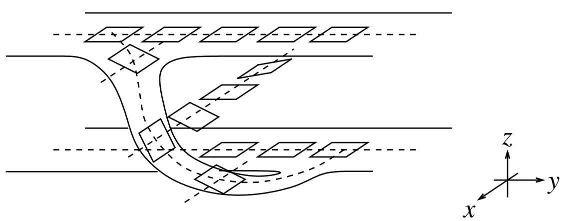

Figure 4. — A positive band of a quasipositive diagram in a position of a Legendrian ribbon.

The main aim of this section is to prove the converse of Lemma 2.1.

THEOREM 2.2. — *A Legendrian ribbon of a Legendrian graph* Γ *in* $(\mathbb{R}^3, \xi_{st})$ *is a quasipositive surface.*

Before proving the assertion, we introduce the notion of backslash position of front projections, trivalent front projections and their approximating fence diagrams.

DEFINITION 2.3. — *A front projection is called in backslash position if all tangent lines lie in* $(\pi/2, \pi) \cup (3\pi/2, 2\pi)$.

Define the diffeomorphism ϕ_1 from the yz-plane to itself by $(y, z) \mapsto (y, \lambda z)$, where $\lambda > 0$ is a positive real number, and the diffeomorphism ϕ_2 as the $-\pi/4$ rotation map of the yz-plane. For a given, Legendrian isotopy move of a front projection, we can choose λ sufficiently small such that the diffeomorphism $\phi_2 \circ \phi_1$ maps all front projections during the move into backslash position.

Definition 2.4. — *A vertex in a generic front projection is called trivalent if the number of adjacent edges is three and two of the edges lie on one side with respect to the vertical line passing through the vertex and the third edge lies on the other side. A front projection is called trivalent if it is generic and all vertices are trivalent.*

Now we consider the local modifications of front projections described in Figure 5. The horizontal and vertical reflections of these modifications are also allowed. The modification in the second line represents a deletion of an edge with a terminal vertex, and the modification in the last line represents a slide of an edge.

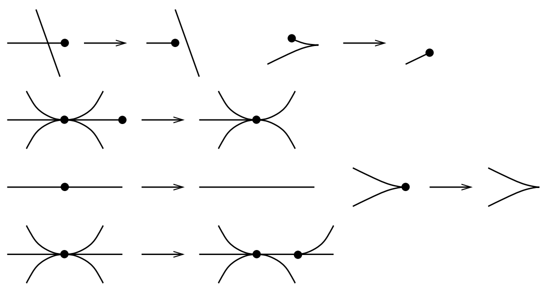

Figure 5. — The local modifications of generic front projections of Legendrian graphs. The horizontal and vertical reflections of these modifications are also allowed.

Lemma 2.5. — *The local modifications in Figure 5 satisfy the following properties:*

(1) the Legendrian ribbons before and after these modifications are ambient isotopic;

(2) every generic front projection can be modified into a trivalent front projection by using these modifications.

Proof. — The assertion (1) can be verified by describing their Legendrian ribbons. For the assertion (2), we can remove an edge with a terminal vertex by using the local modifications in the first and second lines in Figure 5. A vertex with two adjacent edges can be removed by the local modifications in the third line. If a vertex has more than three adjacent edges, we can modify it into a trivalent vertex by iterating the local modifications in the last line. □

Definition 2.6. — *For a fence diagram, we apply deflations as much as possible and then retract each of the left and right ends of horizontal lines* *until their arriving at a trivalent vertex. We call the obtained diagram the reduced fence diagram. See Figure 6. The same operation is also applied to a cusped fence diagram and we call the obtained diagram the reduced, cusped fence diagram.*

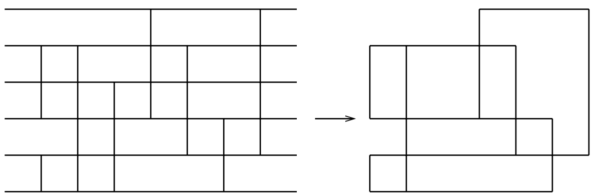

Figure 6. — A reduced fence diagram.

Now we consider to approximate a trivalent front projection in backslash position by reduced fence diagrams. Let q be a fence diagram, r its reduced fence diagram and w a trivalent front projection in backlash position. We denote by $\Sigma_c(r)$ the set of left-top and right-bottom corners of r, which correspond to the cusps in the reduced, cusped fence diagram of q, by $\Sigma_c(w)$ the set of cusps of w, by $\Sigma_n(r)$ and $\Sigma_n(w)$ the set of nodes of r and w respectively, and by $\Sigma_v(r)$ and $\Sigma_v(w)$ the set of trivalent vertices of r and w respectively.

Definition 2.7. — *We say a fence diagram q approximates a trivalent front projection w if its reduced fence diagram r satisfies the following:*

(1) $\Sigma_c(r) = \Sigma_c(w)$;

(2) $\Sigma_n(r) = \Sigma_n(w)$;

(3) $\Sigma_v(r) = \Sigma_v(w)$;

(4) there is a continuous family r_t of curves from $r_0 = r$ to $r_1 = w$, which is polygonal for $t = 0$, such that $r_{t_0} \cap r_{t_1} = \Sigma_c(r) \cup \Sigma_n(r) \cup (r \cap w)$ for all $0 \leqslant t_0 < t_1 \leqslant 1$.

See Figure 7 for example.

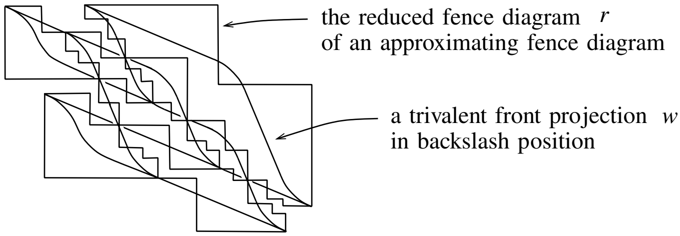

Figure 7. — An example of an approximating fence diagram.

LEMMA 2.8. — *Let q be a fence diagram, r its reduced fence diagram and w a trivalent front projection in backslash position. Suppose that q approximates w. Then*

(1) r is regular isotopic to w as immersed curve in $\mathbb{R}^2$ with cusps, and

(2) the quasipositive surface of the fence diagram q is a Legendrian ribbon of the Legendrian graph of w.

Proof. — It is easy to verify the assertion (1), cf. Figure 7. Isotope the quasipositive surface of the fence diagram q according to the deflations and retractions for making the reduced fence diagram and then isotope it further according to the isotopy move in the assertion (1). We then have a Legendrian ribbon of the Legendrian graph of w. This proves the assertion in (2). □

Proof of Theorem 2.2. — Let $\bar{w}$ be a generic front projection of a given Legendrian graph and assume that $\bar{w}$ is in backslash position. By Lemma 2.5, there exists a trivalent front projection w such that the Legendrian ribbons of w and $\bar{w}$ are ambient isotopic. By Lemma **??**, the Legendrian ribbon of w is quasipositive and hence that of $\bar{w}$ is also. □

3. An alternative proof of Hedden's proposition

Let α be a contact 1-form on S^3 and $\xi = \ker\alpha$ its contact structure. Two manifolds with contact structures are called *contactomorphic* if there exists a diffeomorphism between these manifolds which maps the 2-plane field of the contact structure from one to the other. If ξ is contactomorphic to the contact structure on $S^3 = \{(x_1, y_1, x_2, y_2) \in \mathbb{R}^4 \mid x_1^2 + y_1^2 + x_2^2 + y_2^2 = 1\}$ determined by the kernel of the 1-form $\alpha = \sum_{i=1,2}(x_i dy_i - y_i dx_i)|_{S^3}$, then ξ is called the *standard contact structure* on S^3. In this case, (S^3, ξ) minus one point is contactomorphic to $(\mathbb{R}^3, \xi_{st})$.

Let F be an oriented surface with boundary and $\phi : F \to F$ a diffeomorphism which is the identity map on the boundary ∂F of F. Identify $F \times [0,1]$ by equivalence relations $(x,1) \sim (\phi(x),0)$ for each $x \in F$ and $(y,0) \sim (y,\theta)$ for each $y \in \partial F$ and any $\theta \in [0,1]$. Then F is called a *fiber surface* in the 3-manifold $F \times [0,1]/\sim$. We consider only the case where $F \times [0,1]/\sim$ is S^3. We denote the fiber surface parametrized by $\theta \in [0,1]$ by F_θ and suppose $F = F_0$.

A fiber surface F embedded in S^3 is called *compatible* with a contact structure ξ on S^3 if it satisfies the following:

(1) the boundary of F_θ is transverse to ξ;

(2) $d\alpha$ is a volume form on each fiber F_θ;

(3) the orientation of ∂F_θ coincides with the orientation of ξ determined by $\alpha > 0$.

Theorem 3.1 (Hedden [**?**]). — *Let F be a fiber surface in S^3. F is quasipositive if and only if F is compatible with the standard contact structure on S^3.*

We here give a proof of this theorem without using the affirmative answer to Harer's conjecture.

Proof. — Let F be a fiber surface compatible with the standard contact structure on S^3. By the Legendrian realization argument based on the result in [**?**], we can assume that the fiber surface is a Legendrian ribbon of a Legendrian graph, cf. [**?**, Remark 4.30]. Hence by Theorem 2.2 it is a quasipositive surface.

The proof of the converse assertion is done according to the argument in [**?**, p.21–23]. Let F be a quasipositive surface with a quasipositive diagram. By Lemma 2.1, F can be embedded in S^3 with the standard contact structure ξ_0 in such a way that F is a Legendrian ribbon in (S^3, ξ_0). Since ∂F is transverse to ξ_0, there exists a small tubular neighborhood $N(\partial F)$ of ∂F in S^3 with the contact structure $\ker(dz + r^2 d\theta)$, where the z-coordinate is along ∂F and (r,θ) is the polar coordinates of a plane transverse to ∂F. We then define M to be the union of $F \times [-\varepsilon, \varepsilon]$ and $N(\partial F)$, where ε is a sufficiently small positive real number, and assume that the boundary of M is convex (see [**?**], or for instance [**?**] for the definition of convexity). Since F is a fiber surface, the complement $M^c = \text{closure}(S^3 \setminus M)$ is a handlebody with the tight contact structure $\xi_0|_{M^c}$.

The rest of the proof is the same as the argument in [**?**, p.21–23], so we only show the outline. We first deform the Reeb vector field of (S^3, ξ_0) in such a way that it is tangent to the boundary of $N(\partial F)$ and transverse to the fibers of the fibration in $F \times [-\varepsilon, \varepsilon]$. Next we once forget the contact structure ξ_0 on M^c and extend the Reeb vector field on M to M^c according to the fibration. In particular, the contact structure ξ_1 determined by this Reeb vector field is compatible with the fibration. The Reeb vector field allows us to make a contact embedding of (M^c, ξ_1) into $F \times \mathbb{R}$ with the vertically invariant contact structure. By Giroux's criterion, the contact structure on $F \times \mathbb{R}$ is tight and hence (M^c, ξ_1) is also. The two contact structures $\xi_0|_{M^c}$ and ξ_1 on M^c are both tight and have the same characteristic foliation on ∂M^c. Therefore, due to the uniqueness of the tight contact structure on a handlebody [**?**], we can conclude that the contact structure $(M, \xi_0|_M) \cup (M^c, \xi_1)$ is contactomorphic to (S^3, ξ_0), which is the standard contact structure on S^3. $\square$

4. Isotopy moves of Legendrian graphs and quasipositive diagrams

Definition 4.1. — *Two Legendrian graphs* Γ_0 *and* Γ_1 *in a contact manifold* (M, ξ) *are said to be* Legendrian isotopic *if there exists a one-parameter family* $\{\Gamma_t\}_{t \in [0,1]}$ *of Legendrian graphs from* Γ_0 *to* Γ_1 *such that the cyclic order of adjacent edges tangent to the* 2*-plane of* ξ *at each vertex does not change.*

It is well-known that generic front projections of Legendrian isotopic Legendrian links in $(\mathbb{R}^3, \xi_{st})$ are related by the local moves I, II and III of generic front projections shown in Figure 8 ([**?**]).

Proposition 4.2. — *Generic front projections of Legendrian isotopic Legendrian graphs are related by the local moves described in Figure 8.*

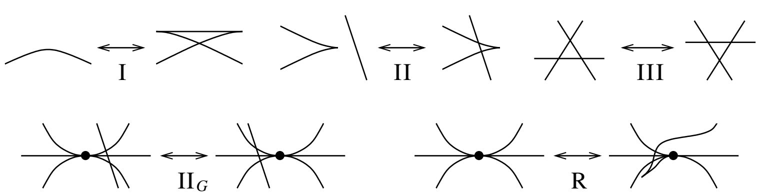

Figure 8. — Legendrian isotopy moves. The horizontal and vertical reflections of these moves are also allowed. The overstrand and understrand at each crossing are determined according to the rule that the arc with the smaller slope passes over the other arc.

Proof. — Let Γ_0 and Γ_1 be two Legendrian graphs, which are Legendrian isotopic, with generic front projections w_0 and w_1 respectively. The Legendrian isotopy $\{\Gamma_t\}_{t \in [0,1]}$ between Γ_0 and Γ_1 is realized by a global move

$\{w_t\}_{t\in[0,1]}$ of front projections from w_0 to w_1. We choose the Legendrian isotopy to be generic so that two vertices do not meet each other in the front projection w_t for each $t \in [0,1]$. We decompose the global move $\{w_t\}_{t\in[0,1]}$ into three kinds of local moves:

(i) no vertex of Γ_t appears in the local move;

(ii) a vertex of Γ_t appears in one of the local moves I, II and III;

(iii) a local move of Γ_t around a vertex which is not in case (ii).

The move in case (i) is realized by a combination of local moves I, II and III. So, we consider the other two cases.

We first consider case (ii). Let v denote the vertex appearing in the local move and ℓ_v denote the line passing through v at which each edge adjacent to v is tangent to ℓ_v. By choosing the Legendrian isotopy $\{\Gamma_t\}_{t\in[0,1]}$ generic, we can assume that the tangency to ℓ_v of each adjacent edge does not change during this local move. Then it is clear that both of the local moves II and III with a vertex can be realized as a combination of the local moves II_G described in Figure 8. In case of the local move I with a vertex, we decompose the Legendrian isotopy move into two steps: we first keep the vertex outside the triangle in the right of the move I, and then move it into somewhere on the boundary of the triangle if necessary. The first move is just the local move I, and the second move can be realized as a combination of the local move II_G and some move around a cusp. This last move is considered to be in case (iii).

Next we consider case (iii). Since each edge adjacent to the vertex v is Legendrian, we can label these edges by $e_1, \cdots, e_m$ in such a way that

(1) $e_1, \cdots, e_m$ are ordered in anti-clockwise orientation with respect to ξ,

(2) $e_1, \cdots, e_k$ lie on the left of the vertex v in the generic front projection and $e_{k+1}, \cdots, e_m$ lie on the right,

see Figure 9. Since the Legendrian move in case (iii) keeps the property that these edges are Legendrian, the move which can appear is only a rotation of one of the edges e_1, e_k, e_{k+1}, e_m onto the other side of the vertex v, keeping the order fixed in (1). Such a rotation is realized by the local move R described in Figure 8. Remark that a local move where a vertex passes though a cusp is also realized by this rotation. This completes the proof. □

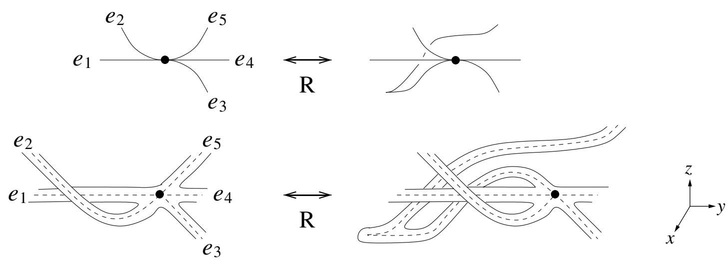

Figure 9. — Label adjacent edges in anti-clockwise orientation with respect to ξ, and rotate one of the edges onto the other side.

Theorem 4.3. — *If the Legendrian graphs of reduced, cusped fence diagrams are Legendrian isotopic, then their fence diagrams are related by inflations, deflations, slips and slides.*

*Remark 4.4. — In [**?**], the slides were defined as the moves from the left to the right in Figure 3 and it was remarked on p.263 that the inverse moves can be realized as conjugations of slides by twirls. In this paper, for our convenience to compare with Legendrian isotopy moves, we call these inverse moves also slides. The definitions of twirls and turns in Figure 3 are also different from those in [**?**] because of the same reason.*

Before proving Theorem **??**, we explain the flexibility of approximating fence diagrams shown in Figure 10. The thickened polygonal curves in the figures represent a part of the reduced fence diagram. Figure (A) shows that by combining an inflation and a slide we can produce a fence diagram with better approximation. Figure (B) shows that by combining an inflation, slides and a deflation we can exchange the heights of two horizontal edges, and Figure (C) shows that by a slip we can exchange the positions of vertical edges. These properties imply that we can make an approximating fence diagram whose reduced fence diagram is as close to w as we need by using inflations and slides, and every regular isotopy move of a generic front projection, as moves of immersed curves in $\mathbb{R}^2$ with cusps, can be expressed by a family of approximating fence diagrams defined by inflations, deflations, slips and slides.

Proof of Theorem **??**. — We first show that the Legendrian isotopy moves I, II, III, II_G, R can also be expressed by moves of approximating fence diagrams. Since all reduced fence diagrams are trivalent, the vertices in the moves II_G, R are trivalent. Consider the move II with right cusp. If the cusp passes a line from the top to the bottom, then the move is expressed by a combination of an inflation and slides as shown on the top in Figure 11.

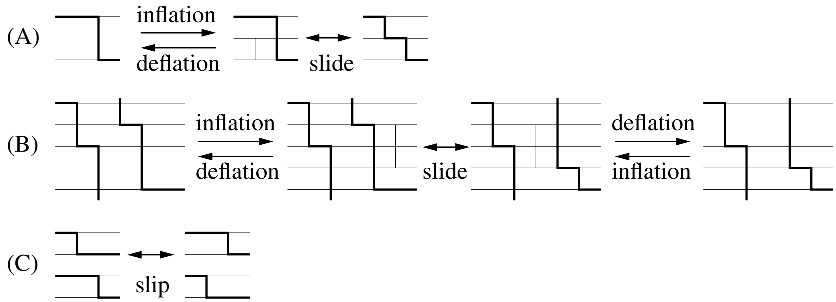

Figure 10. — Flexibility of approximating fence diagrams.

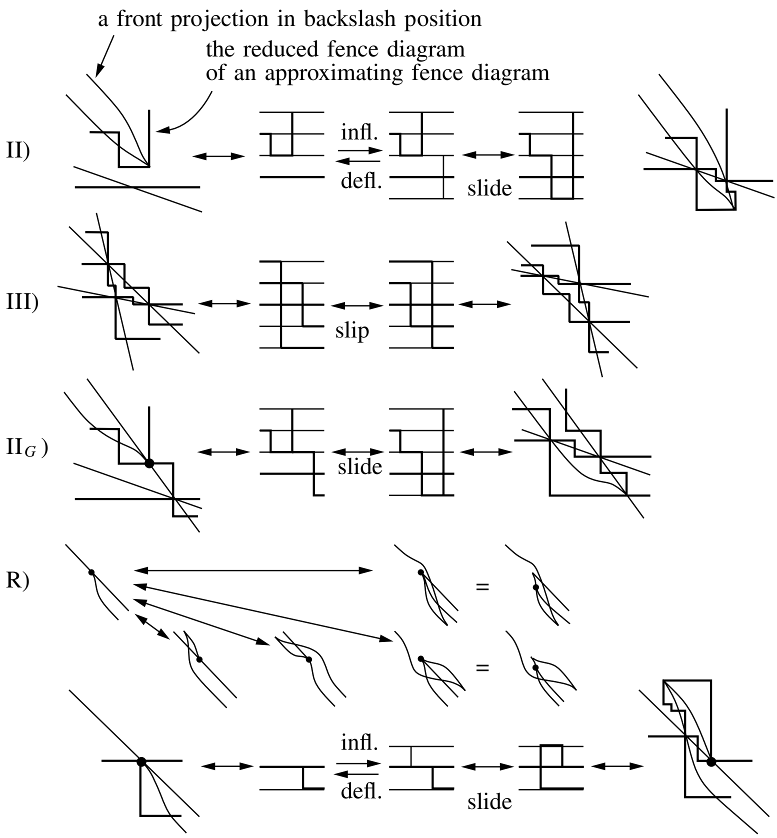

Figure 11. — The moves of approximating fence diagrams corresponding to the Legendrian isotopy moves II, III, II$_G$, R.

The move of approximating fence diagrams corresponding to the move II with left cusp is given by the π-rotation of the figure. In case the right (resp. left) cusp passes a line from the left to the right (resp. from the right to the left), the move corresponds to a slip, cf. Figure 12 below. For every move which appears below, we also need to check the figure obtained by the π-rotation, though we omit it. The move III corresponds to a slip, which is shown on the second figure in Figure 11. The move II_G corresponds to a slide if the cusp passes a line from the top to the bottom, see the third figure. In case where the cusp passes a line from the left to the right, the move corresponds to a slip. The move R has four cases as shown in the fourth figure. The move of approximating fence diagrams for the first case is shown on the bottom in Figure 11. Looking only at the cusp in the move R on the bottom in Figure 11, we have the move I. We can check the other cases of the move R by the same way. Thus we conclude that all the moves I, II, III, II_G, R are expressed by approximating fence diagrams with using inflations, deflations, slips and slides.

Now we prove the assertion. Let w and w' be reduced, cusped fence diagrams whose Legendrian graphs are Legendrian isotopic and r_0 and r_0' the reduced fence diagrams corresponding to w and w' respectively. By small perturbation we can assume that w and w' are in backslash position, and by applying move (A) in Figure 10 to r_0 and r_0' we can obtain fence diagrams r_1 and r_1' which approximate w and w' respectively. Now we make the approximation r_1 of w as close to w as possible and follow the Legendrian isotopy moves from w to w' with approximating fence diagrams. We denote the obtained fence diagram by r_2, which approximates w'. It is easy to make the same approximation of w' from r_1' and r_2 by applying move (A) in Figure 10. Thus r_0 and r_0' are related by the moves in the assertion.

5. Quasipositive annuli

In this section we study quasipositive annuli. The reduced fence diagram of a quasipositive diagram of a quasipositive annulus has no trivalent vertices, i.e., it is a knot diagram of a knot in $\mathbb{R}^3$.

Theorem 5.1. — *The moves of fence diagrams of quasipositive annuli under inflation, deflation, slips and slides correspond to Legendrian isotopy moves of reduced, cusped fence diagrams.*

Proof. — An inflation and a deflation do not change the reduced fence diagram. The slip of a reduced fence diagram shown in Figure 12 corresponds to the Legendrian move II if there is no horizontal line passing under the shorter vertical edge. In case where the shorter vertical edge passes over several horizontal lines, the move is realized by the moves II and III. The other cases of slips are obviously Legendrian isotopy.

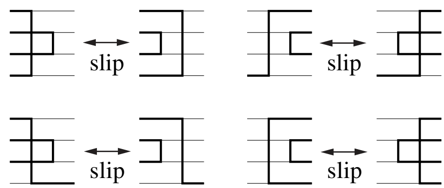

Figure 12. — Moves of reduced fence diagrams under slips.

We consider the slide from the left to the right shown in Figure 13 (A). If the reduced fence diagram does not pass through the lower vertical edge in Figure 13 (B), then this move is obviously Legendrian isotopy. If it passes through the lower vertical edge, there are eight cases shown in Figure 13 (C). The non-obvious case is (C3) and corresponds to the Legendrian isotopy move I. In case where the vertical lines of fence diagrams in Figure 13 pass over several other horizontal lines, we may need to use the Legendrian isotopy move II additionally. The proof for the slide from the right to the left also follows from Figure 13. For the second slide in Figure 3, the proof is analogous. □

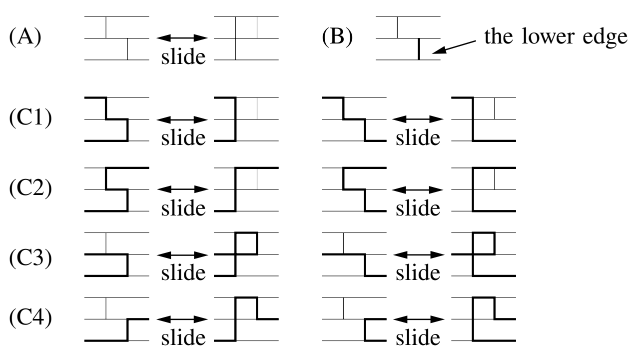

Figure 13. — Moves of reduced fence diagrams under slides.

Remark 5.2. — For quasipositive surfaces, the moves of their fence diagrams under inflation, deflation and slips correspond to Legendrian isotopy moves of reduced, cusped fence diagrams. But this is not true for slides. Figure 14 shows that a slide may exchange the mutual positions of two vertices and this cannot be realized by Legendrian isotopy moves of Legendrian graphs.

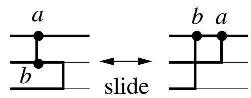

Figure 14. — A slide which exchanges the mutual positions of two vertices.

Remark 5.3. — Theorem **??** shows the existence of the surjective map

$$\{\text{trivalent Legendrian ribbons}\}_{/\sim} \to \{\text{quasipositive diagrams}\}_{/\sim},$$

where $\{\text{trivalent Legendrian ribbons}\}_{/\sim}$ is the class of Legendrian graphs up to Legendrian isotopy and $\{\text{quasipositive diagrams}\}_{/\sim}$ is the class of quasipositive diagrams up to inflations, deflations, slips, slides, twirls and turns, and the above remark shows that this map is not injective.

6. Quasipositive surfaces with different fence diagrams

Let γ be a Legendrian knot in $(\mathbb{R}^3, \xi_{st})$, i.e., γ is tangent to the 2-plane field ξ_{st} everywhere. The *Thurston-Bennequin invariant* $tb(\gamma)$ of γ is the linking number of γ and a curve obtained by pushing off γ normal to ξ_{st}. To give the definition of the rotation number, we assign an orientation to γ and denote it by $\vec{\gamma}$. The *rotation number* $r(\vec{\gamma})$ of $\vec{\gamma}$ is the winding number of vectors tangent to $\vec{\gamma}$ with respect to the trivialization of ξ_{st} along $\vec{\gamma}$. The other choice of the orientation of γ changes the sign of the rotation number.

The Thurston-Bennequin invariant and the rotation number can be read from the front projection. Let γ be a Legendrian knot and w_γ its generic front projection. Assign an orientation to w_γ and let $p(w_\gamma)$ (resp. $n(w_\gamma)$) denote the number of positive (resp. negative) crossings and $r_c(w_\gamma)$ the number of right cusps of w_γ. Then the Thurston-Bennequin invariant of γ is determined by the formula

$$tb(\gamma) = p(w_\gamma) - n(w_\gamma) - r_c(w_\gamma). \tag{6.1}$$

Obviously, this number does not depend on the choice of the orientation. For the rotation number, let $d_c(w_\gamma)$ (resp. $u_c(w_\gamma)$) denote the number of downward (resp. upward) cusps. Then the rotation number is determined by

$$r(\vec{\gamma}) = \frac{1}{2}(d_c(w_\gamma) - u_c(w_\gamma)).$$

It is easy to verify that the other choice of the orientation of γ changes the sign of the rotation number. For more precise explanations, see for instance [**?**].

A reduced, cusped fence diagram of a quasipositive annulus is regarded as a front projection of a Legendrian knot. We define the Thurston-Bennequin invariant and the rotation number of a fence diagram of a quasipositive annulus by those of its reduced, cusped fence diagram.

LEMMA 6.1. — *The Thurston-Bennequin invariant of a fence diagram of a quasipositive annulus A is equal to -1 times the linking number of the two boundary components of A. In particular, the Thurston-Bennequin invariant is independent of the choice of a quasipositive diagram.*

Proof. — On a quasipositive diagram, we assume that the positive crossing of each positive band lies close to the bottom end of the band. Then the contribution to the linking number of the two boundary components of A is given as shown in Figure 15. The number on the right-bottom of each figure represents the contribution to the linking number. Thus the linking number is $-p+n+r_c=-tb$ by formula (6.1). □

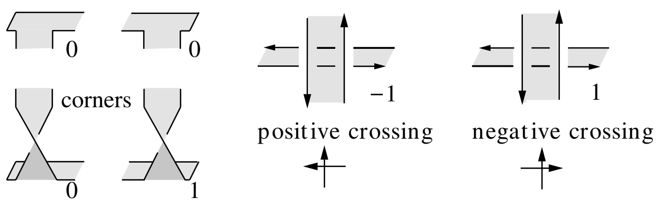

Figure 15. — The contribution to the linking number of the two boundary components of A.

Remark 6.2. — Lemma **??** can be proved by checking the coincidence of the Legendrian framing and the Seifert surface's framing of a reduced, cusped fence diagram, cf. for example [**?**]. This proof is more direct than the above proof if we assume the knowledge of these framings.

THEOREM 6.3. — *The Thurston-Bennequin invariant and the rotation number of a fence diagram of a quasipositive annulus are invariant under inflations, deflations, slips, slides, twirls and turns.*

Proof. — Since the moves of quasipositive annuli in the assertion are ambient isotopy moves of Seifert surfaces, the linking number of the two boundary components of a quasipositive annulus does not change under these moves. Therefore, by Lemma **??**, the Thurston-Bennequin invariant also does not change. The rotation number is also invariant under inflations, deflations, slips and slides since they are Legendrian isotopy moves by Theorem **??**.

We will prove the invariance of the rotation number in case of twirls and turns. For twirls, there are four cases (A), (B), (C) and (D) of reduced fence diagrams as shown in Figure 16. We assign an orientation as shown in the figures. The small arrows in the figures represent the positions of upward and downward cusps. It is easy to check that the rotation number does not change under these moves. The other choice of the orientation changes the sign of the rotation number, but it does not matter for its invariance under these moves.

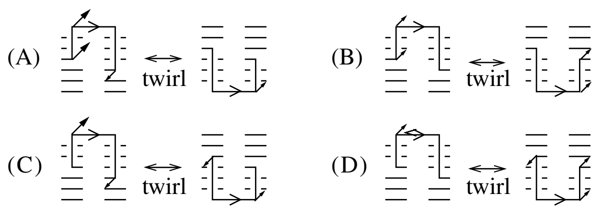

Figure 16. — The four cases of the moves of reduced fence diagrams under twirls.

The proof of the invariance under turns is analogous to the proof for twirls. There are four cases (A), (B), (C) and (D) of the moves of reduced fence diagrams as shown in Figure 17 and we can check easily that the rotation number does not change under these moves. □

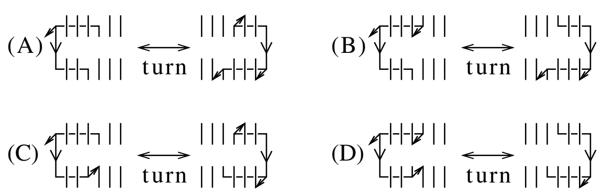

Figure 17. — The four cases of the moves of reduced fence diagrams under turns.

As a corollary, we answer a question of Rudolph in [**?**, Remark in p.263].

Corollary 6.4. — *There exists a quasipositive surface with two different quasipositive diagrams which are not related by inflations, deflations, slips, slides, twirls and turns.*

Proof. — We consider two fence diagrams shown in Figure 18. They are quasipositive annuli and it is easy to check by formula (6.1) that the Thurston-Bennequin invariants are both -3. Hence, by Lemma **??**, their quasipositive surfaces are the same, namely the 3 times full twisted quasipositive annulus. However the rotation number of the fence diagram on the left is 0 and the number of the right diagram is ± 2. Hence, by Theorem **??**, these fence diagrams are not related by the moves in the assertion. □

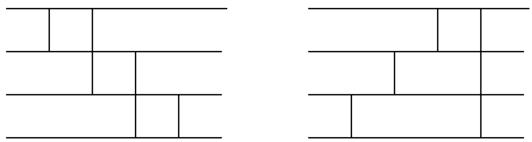

Figure 18. — Two different fence diagrams of the 3 times full twisted quasipositive annulus.

If the Legendrian isotopy class of a Legendrian knot with the same knot-type is determined by the Thurston-Bennequin invariant and the rotation number, then this knot-type is called *Legendrian simple*. It is known by Y. Eliashberg and M. Fraser in [**?**] that the unknot is Legendrian simple, and J. Etnyre and K. Honda proved in [**?**] that the torus knots and the figure eight knot are Legendrian simple. On the other hand, the knots 5_2, 6_3 and 7_2, in Rolfsen's notation [**?**], are not Legendrian simple [**?**, **?**]. These facts are known as an application of Chekanov's differential graded algebra [**?**].

As a direct corollary of Theorem **??**, we can determine the isotopy class of a quasipositive annulus up to the moves of quasipositive annuli in case where its core curve is Legendrian simple.

Corollary 6.5. — *Let A be a quasipositive annulus such that the knot type of its core curve is Legendrian simple.*

(1) The isotopy class of a quasipositive diagram of A up to inflations, deflations, slips and slides is determined by the Thurston-Bennequin invariant and the rotation number of their reduced, cusped fence diagrams.

(2) The classification of quasipositive diagrams of A in (1) is equivalent to the classification up to inflations, deflations, slips, slides, twirls and turns.

For example, consider the n times full twisted quasipositive annulus A_n. By using the classification of the Legendrian unknot in [**?**], we know that there exist $\lfloor (n+1)/2 \rfloor$ reduced fence diagrams of A_n with different rotation numbers. Hence, by Corollary **??**, we conclude that they are not related by inflations, deflations, slips, slides, twirls and turns.

Remark 6.6. — The existence of the map

$$\{\text{quasipositive diagrams}\}_{/\sim} \to \{\text{quasipositive surfaces}\}_{/\sim}$$

is obvious and Corollary **??** shows that this map is not injective, where $\{\text{quasipositive surfaces}\}_{/\sim}$ is the class of quasipositive surfaces up to ambient isotopy and $\{\text{quasipositive diagrams}\}_{/\sim}$ is the class of quasipositive diagrams up to inflations, deflations, slips, slides, twirls and turns.

Remark 6.7. — In the preliminary version of this paper, we asked whether there exists a quasipositive fiber surface, other than a disk, from which we cannot deplumb a Hopf band. M. Hirasawa informed us later that the $(2,1)$-cable of the right-handed trefoil satisfies this property, and M. Hedden also pointed out the same fact in [**?**] independently.

Acknowledgements. — This work was done while the second author visited Forschungsinstitut für Mathematik of ETH Zürich and Mathematisches Institut of Universität Basel during the summer semester in 2006. He would like to thank the staff of these departments, especially Norbert A'Campo, for their warm hospitality and precious support. He is supported by MEXT, Grant-in-Aid for Young Scientists (B) (No. 16740031) during this work.

Bibliography

[1] Akbulut (S.), Ozbagci (B.). — Lefschetz fibrations on compact Stein surfaces, Geometry & Topology 5, p. 319-334 (2001).

[2] Chekanov (Y.). — Differential algebra of Legendrian links, Invent. Math. 150, p. 441-483 (2002).

[3] Eliashberg (Y.), Fraser (M.). — Classification of topologically trivial Legendrian knots, in Geometry, topology, and dynamics (Montreal, PQ, 1995), pp. 17-51, CRM Proc. Lecture Notes 15, A.M.S., Providence, RI, (1998).

[4] Etnyre (J.B.). — Lectures on open book decompositions and contact structures, Floer homology, gauge theory, and low-dimensional topology, pp. 103-141, Clay Math. Proc., 5, A.M.S., Providence, RI, 2006.

[5] Etnyre (J.B.), Honda (K.). — Knots and contact geometry. I. Torus knots and the figure eight knot, J. Symplectic Geom. 1, p. 63-120 (2001).

[6] Giroux (E.). — Convexité en topologie de contact, Comment. Math. Helvetici 66, p. 637-677 (1991).

[7] Giroux (E.). — Géométrie de contact : de la dimension trois vers dimensions supérieures, Proceedings of the International Congress of Mathematicians, Vol II (Beijing, 2002), pp.405-414, Higher Ed. Press, Beijing, (2002).

[8] Gompf (R.E.). — Handlebody construction of Stein surfaces, Ann. of Math. 148, p. 619-693 (1998).

[9] Goodman (N.). — Contact structures and open books, Ph. D thesis, UT Austin, (2003).

[10] Harer (J.). — How to construct all fibered knots and links, Topology 21, p. 263-280 (1982).

[11] Hedden (M.). — Notions of positivity and the Ozsváth-Szabó concordance invariant, to appear in J. Knot Theory Ramifications, available at: arXiv.math.GT/0509499.

[12] Hedden (M.). — Some remarks on cabling, contact structures, and complex curves, to appear in Proc. Gökova Geom. Topol. Conference, 2007, available at: arXiv.math.GT/0804.4327.

[13] Ng (L.L.). — Computable Legendrian invariants, Topology 42 (2003), no. 1, 55-82.

[14] D. Rolfsen, Knots and links, Mathematics Lecture Series 7, Publish or Perish, Inc., Berkeley, Calif., (1976).

[15] Rudolph (L.). — Quasipositive plumbing (Constructions of quasipositive knots and links, V), Proc. A.M.S. 126, p. 257-267 (1998).

[16] Światkowski (J.). — On the isotopy of Legendrian knots, Ann. Glob. Anal. Geom. 10, p. 195-207 (1992).

[17] Torisu (I.). — Convex contact structures and fibered links in 3-manifolds, Int. Math. Res. Not. 9, p. 441-454 (2000).